The 2010 IEEE/RSJ International Conference on
Intelligent Robots and Systems
October 18-22, 2010, Taipei, Taiwan

An Asymmetric Stiffness Model of a Human Hand

Satoko Abiko, Atsushi Konno and Masaru Uchiyama
Dept. of Aerospace Engineering
Tohoku University
Aramaki-aza Aoba 6-6-01, Sendai, 980-8579, Japan
satoko.abiko@ieee.org

***Abstract*— This paper presents an asymmetric stiffness characteristic of a human hand. In human support robotics or medical robotics, the detail comprehension of physical human body is important to develop safe and high performed robots to work cooperatively with a human and to replace human dexterous tasks. It is known that a human arm generates variable stiffness depending on tasks by coactivation of agonist and antagonist muscles. Previous related researches have been presented impedance characteristics of a human upper limb in static posture and dynamic motion. These characteristics are represented by ellipsoids. However, the above analyses are based on a simple muscle model and conventional kinematic and dynamics of an articulated body system. In this paper, perturbation-excited method is carried out for estimating the stiffness of a human hand. The experimental results demonstrate nonlinear property of the stiffness of a human hand. To illustrate the observed stiffness characteristic, this paper proposes nonlinear stiffness model of the human hand.**

***Index Terms*— viscoelasticity, variable stiffness, asymmetric stiffness, perturbation-excited method.**

I. INTRODUCTION

The application of robotic technologies is expanding to new fields. Human support robots or medical robots in rehabilitation and surgical operation are expected to perform dexterous tasks in cooperation with a human and to replace human in tasks. Such robots require capability to reproduce the dexterous skill of human or to be safe in the interaction between the human. To establish such robotic technology from both mechanical and control aspects, the comprehension of the dexterous skill and adaptive learning in arbitrary tasks of a human is of importance. This analysis can enhance the possibility of human-robot safe interactive work and give new insight to design and develop a novel robot.

This paper presents an asymmetric stiffness characteristic of a human hand. To estimate the stiffness of a human hand, the perturbation excited experiment is carried out. The experimental results demonstrate nonlinear stiffness characteristic of the human hand. It is known that the human can change the viscoelasticity of her/his hand during movement or even in static posture. The previous related researches represented such stiffness or impedance characteristics of a human hand as symmetric ellipsoids in certain tasks [1]–[6]. These symmetric ellipsoids can be illustrated by a simple muscle model (*e.g. Hill's model*) and coordinate mapping among the joint space, muscle space, and operational space.

However, when the stiffness estimation experiment was carried out by exciting the perturbation on the human hand, we observed an asymmetric stiffness characteristic on the human hand. The aforementioned simple muscle model cannot describe such a property. To comprehend the observed stiffness property, this paper proposes an asymmetric stiffness model in a muscle model. Then, the stiffness model of a human hand is analyzed by the proposed model in two dimensional case. In the analysis, an upper limb of the human arm is modeled with one pair of biarticular muscles and two pairs of simple joint muscles. This paper also presents the experimental results of the stiffness estimation. The experiment was carried out to identify the stiffness in three dimension in certain static posture.

This paper is organized as follows. Section II reviews previous related researches including estimation of viscoelasticity and stiffness of a human hand in movement and in static posture. Section III proposes a new muscle model with asymmetric stiffness characteristic. In this section, dynamics of the upper limb is also explained. Section IV shows numerical analysis of the stiffness characteristic of the human hand with asymmetric stiffness model. Section V demonstrates perturbation-based stiffness estimation and discusses the estimated stiffness characteristics by comparing with the proposed muscle model. The paper is summarized in Section VI.

II. BIBLIOGRAPHY

In the field of man-machine cooperation system, Kosuge *et. al.* roughly identified impedance parameters of a human operator with a simple one degree-of-freedom manipulandum system. They used the estimated parameters to realize desired interaction between the environment and the operator. However, they focused on the performance analysis of the integrated man-machine system. Therefore, they estimated one set of parameters without considering the influence of the change of the arm posture and muscle activation [7]. Asada and Asari also identified impedance characteristics of the human hand while the human is handling a tool to guide curved surface. They implemented the parameters for the direct teaching in [8]. Their aim was to implement dexterous skill of the human into the robot via the direct teaching. However, they did not contemplate the detail clarification of the human impedance characteristics.

On the other hand, many researches have investigated the function of central nervous system and physical characteristics of the human body itself [1]–[6]. Hogan modeled an

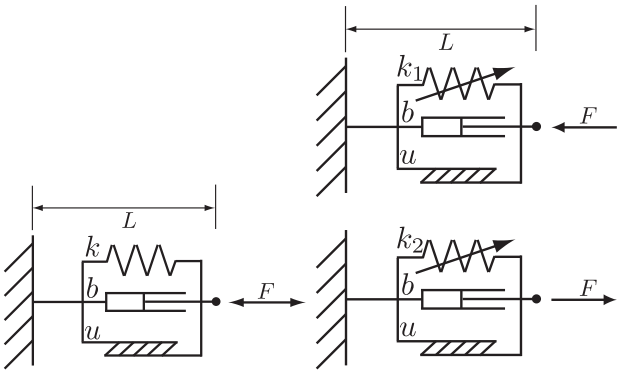

(a) Symmetric model (b) Asymmetric model

Fig. 1: Muscle model

upper limb of the human arm with simple muscle model and introduced the representation of the stiffness characteristic of the human hand as an ellipsoid [1], [9]. By following the above idea, the impedance characteristics are estimated in static posture with the least-square parameter fitting method in [2], [6]. They presented that the impedance characteristics of the human hand are dependent on the posture of the human hand. However, generally the estimation of the viscosity is difficult to identify. Therefore, some researches focused on the stiffness estimation instead of whole impedance characteristics since the stiffness is of importance for the human arm to be stable in arbitrary tasks [3]. In [3] and [4], it has been shown that the stiffness are variable according to the ratio of the muscle activation. They described the above variable stiffness characteristic of the human arm as a symmetric ellipsoid.

However, the stiffness estimation we conducted demonstrated that the stiffness property is variable according to the direction of the perturbation even in the same posture. This paper presents an asymmetric stiffness characteristic of the human hand and proposes a new stiffness model of the muscle model to describe the observed property.

III. MODELING OF MUSCLE AND HUMAN ARM

First, the well-known Hill's muscle model is reviewed. The Hill's model generally expresses the constant stiffness coefficient derived as a function of the motor command (*e.g. motoneuronal activations*) in the isometric condition. In order to explain an asymmetric stiffness characteristic on the human hand obtained in the perturbation-based stiffness estimation in Section V, this section proposes an asymmetric stiffness model. Thereafter, the stiffness of the muscle is described by the asymmetric stiffness model.

A. Muscle model

The muscle tension F is determined as the following Hill's model:

$$F = u(\alpha) - K(\alpha)(L_0 - L) - B(\alpha)\frac{dL}{dt}, \qquad (1)$$

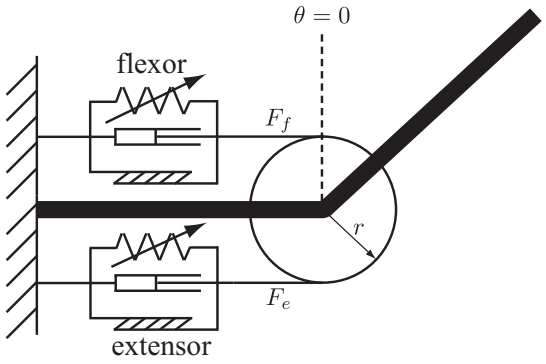

Fig. 2: Antagonistic muscle model with asymmetric muscle model

where α represents the motor command, which is normalized by the maximum motor command level. Therefore, the range of the motor command is:

$$0 \leq \alpha \leq 1. \qquad (2)$$

L and $\frac{dL}{dt}$ represent muscle length and contraction velocity of the muscle, respectively. L_0 denotes the intrinsic muscle length. $u(\alpha) = \alpha f_0$ represents contraction force, in which f_0 is the maximum tension in the isometric contraction at the intrinsic length of muscle. $K(\alpha)$, $B(\alpha)$ represent muscle stiffness and viscosity, respectively. These values are generally nonlinear in terms of the motor command. Here, let these values assumed to be linear in terms of the motor command as follows:

$$K(\alpha) = k_0 + k\alpha, \qquad (3)$$

$$B(\alpha) = b_0 + b\alpha, \qquad (4)$$

where k_0 and b_0 are intrinsic stiffness and viscosity. k and b express the stiffness and viscosity coefficients, respectively.

In the conventional muscle model, the stiffness coefficient k is assumed to be constant and only the motor command α changes the total stiffness characteristic. This paper proposes the following asymmetric stiffness model.

$$K(\alpha) = \begin{cases} k_0 + k_1\alpha & (\ F \geq 0 \ or \ (L_0 - L) \leq 0\ ) \\ k_0 + k_2\alpha & (\ F < 0 \ or \ (L_0 - L) > 0\ ) \end{cases}, \qquad (5)$$

where the switching conditions are dependent on the perturbation direction. For example, if the perturbation is applied to the direction of extension of the muscle, $K(\alpha) = k_0 + k_1\alpha$. This model enables the stiffness coefficient K itself to change depending on the contraction or extension of the muscle. Fig. 1 illustrates the difference between the conventional symmetric stiffness model and the proposed asymmetric stiffness model.

B. Antagonistic muscle model with the asymmetric stiffness characteristic

The model of the coactivation of flexor and extensor muscles is simply formed with the aforementioned muscle model. Fig. 2 shows a simple model to manipulate one degree-of-freedom (DOF) joint with the flexor and extensor

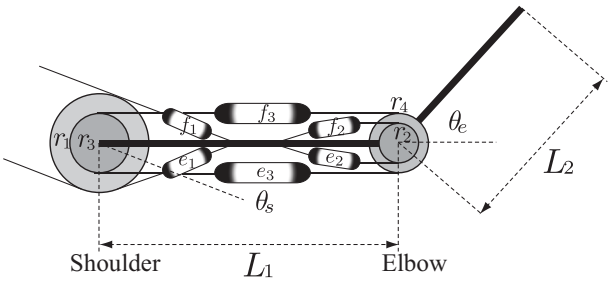

Fig. 3: Dynamic model of the human limb with four single-joint muscles and two double-joint muscles

muscles. The joint torque τ is generated by both muscles as follows:

$$\begin{aligned}\tau &= r\big(F_f - F_e\big) \\ &= \{u_f(\alpha_f) - u_e(\alpha_e)\}r \\ &- \{K_f(\alpha_f) + K_e(\alpha_e)\}r^2\theta - \{B(\alpha_f) + B(\alpha_e)\}r^2\dot{\theta},\end{aligned} \tag{6}$$

where $r\theta = L_0 - L$ is applied. In (6), the stiffness model is the asymmetric muscle model as:

$$K_i(\alpha_i) = \begin{cases} k_0 + k_1\alpha_i & (\ F_i \geq 0\ ) \\ k_0 + k_2\alpha_i & (\ F_i < 0\ ) \end{cases} \quad (\ i = f \text{ or } e\ ).$$

The subscript f and e express the flexor and the extensor.

Let (6) to be linearized around an equilibrium point in a certain isometric condition with a certain activity level of the motor command as:

$$\frac{\delta\tau}{\delta\theta} = -\{K_f(\alpha_f) + K_e(\alpha_e)\}r^2. \tag{7}$$

Equation (7) implies that the muscle stiffness is mapped to the stiffness in joint space. Note that the activity level of the motor command changes the stiffness characteristic as many previous related researches suggested. However, (7) expresses that only the change of the activity level of the motor command can not express the asymmetry of the stiffness since the stiffness characteristic does not change when the deflection is applied to the different direction in the case of the symmetric stiffness model. Therefore, the asymmetric muscle model is required to express the asymmetric stiffness characteristic.

C. Upper limb model of a human arm

The skeletal muscle system of an upper limb of a human arm contains four simple joint muscles and two biarticular muscles. The two pairs of simple joint muscles and one pair of biarticular muscles are antagonistic. The extension of the antagonistic muscle model mentioned in the previous subsection provides the upper limb model of the human arm with the asymmetric stiffness characteristic. The upper limb model of the human arm is illustrated in Fig. 3. The torques applied to the shoulder and the elbow joints are determined with the motor activations, stiffness, and viscosity of the muscles as follows:

$$\boldsymbol{\tau} = \boldsymbol{U}_\theta + \boldsymbol{K}_\theta\boldsymbol{\theta} + \boldsymbol{B}_\theta\dot{\boldsymbol{\theta}}, \tag{8}$$

TABLE I: Muscle parameters

		k $[N/m]$	k_0 $[N/m]$	b $[N\cdot s/m]$	b_0 $[N\cdot s/m]$
flexor	k_1	1621.6	810.8	108.1	54.1
	k_2	520.0	810.8	108.1	54.1
extensor	k_1	1621.6	810.8	108.1	54.1
	k_2	520.0	810.8	108.1	54.1

TABLE II: Parameters of muscle length

	$r[m]$	$L_0[m]$
Shoulder flexor	-0.03491	0.09076
Shoulder extensor	0.03491	-0.02793
Elbow flexor	-0.02182	-0.05672
Elbow extensor	0.02182	0.00436
Biarticular flexor	-0.05498	0.14294
Biarticular extensor	0.05498	-0.01343

TABLE III: Kinematic and dynamic parameters of arm

	$m[kg]$	$L[m]$	$L_g[m]$	$I[kgm^2]$
Link 1	1.59	0.30	0.18	0.0477
Link 2	1.44	0.35	0.21	0.0588

TABLE IV: Moment arms

	r_1	r_2	r_3	r_4
Moment arm [m]	0.040	0.025	0.028	0.035

where

$$\boldsymbol{\tau} = \begin{bmatrix} \tau_s \\ \tau_e \end{bmatrix}, \quad \boldsymbol{\theta} = \begin{bmatrix} \theta_s \\ \theta_e \end{bmatrix},$$

$$\boldsymbol{U}_\theta = \begin{bmatrix} \Delta u_1 r_1 + \Delta u_3 r_3 \\ \Delta u_2 r_2 + \Delta u_3 r_4 \end{bmatrix}, \quad \Delta u_j = u_{f_j} - u_{e_j},$$

$$\boldsymbol{K}_\theta = \begin{bmatrix} -K_1 r_1^2 - K_3 r_3^2 & -K_3 r_3^2 \\ -K_3 r_4^2 & -K_2 r_2^2 - K_3 r_4^2 \end{bmatrix},$$

$$\boldsymbol{B}_\theta = \begin{bmatrix} -B_1 r_1^2 - B_3 r_3^2 & -B_3 r_3^2 \\ -B_3 r_4^2 & -B_2 r_2^2 - B_3 r_4^2 \end{bmatrix}.$$

In the above, $K_j = K_{f_j}(\alpha_{f_j}) + K_{e_j}(\alpha_{e_j})$ and $B_j = B(\alpha_{f_j}) + B(\alpha_{e_j})$ $(j = 1, 2, 3)$. Note here that K_j switches its value according to the asymmetric muscle stiffness as described in (5). Therefore, the viscoelasticity of the human hand are determined by the combination of the motor command α of each joint and the muscle stiffness condition.

Let (8) to be linearized around an equilibrium point in a certain isometric condition with a certain activation level of the motor command as:

$$\frac{\delta\boldsymbol{\tau}}{\delta\boldsymbol{\theta}} = \boldsymbol{K}_\theta. \tag{9}$$

Equation 9 describes the stiffness in joint space which is expressed by the muscle stiffness. Note that this paper models the moment arms of the pairs of muscles are assumed to be equal. The different moment arms of the pairs of muscles would be a more detail model of the muscle configuration of the human arm. However, even in the detail model of the muscle configuration, the asymmetric stiffness characteristics can be expressed only with the asymmetric stiffness condition as shown in (5).

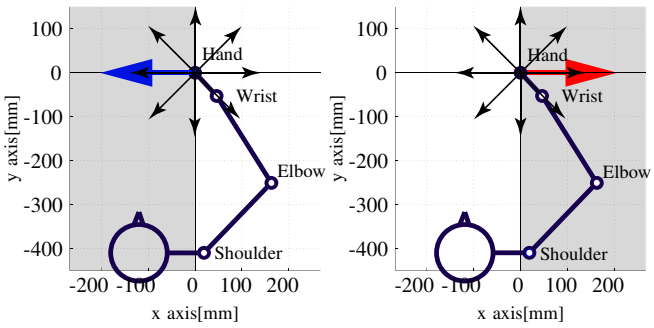

Fig. 4: Force direction applied by a human

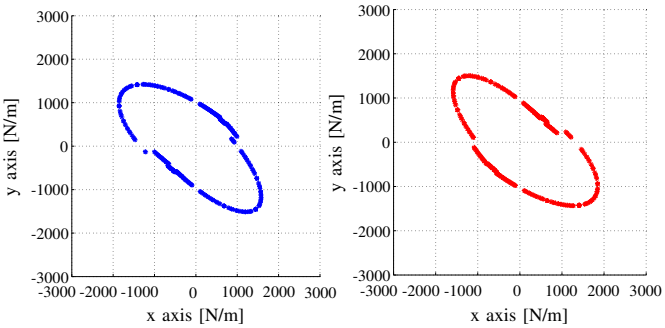

Fig. 5: Asymmetric stiffness ellipses in the simulation

D. Stiffness of a human hand

The stiffness property of a human hand is a mapped stiffness of the muscle and skeletal stiffness property. In the isometric condition, the stiffness of the human arm becomes a function of the posture of the human arm and the stiffness in joint space as follows:

$$\boldsymbol{K}_h = \left(\boldsymbol{J}\boldsymbol{K}_\theta^{-1}\boldsymbol{J}^T\right)^{-1}, \tag{10}$$

where $\boldsymbol{K}_h$ and $\boldsymbol{K}_\theta$ denote the stiffness matrices on the hand and in the joint space, respectively. The stiffness of the joint space is also generated by the muscle stiffness. $\boldsymbol{J}$ denotes the Jacobian matrix between the joint space and the operational space. As shown in (10), $\boldsymbol{K}_h$ is a quadratic function of Jacobian matrix and scaled by the stiffness of the joint space that is the mapped stiffness from the muscle stiffness model. Hence, the asymmetric stiffness characteristic of the human hand is dependent on only the muscle stiffness model.

The stiffness matrix of a human hand expresses the relationship between the small perturbation onto the hand $\delta\mathcal{F}_h \in \Re^{3\times1}$ and the displacement of the human hand $\delta\boldsymbol{p}_h \in \Re^{3\times1}$.

$$\delta\mathcal{F}_h = \boldsymbol{K}_h\delta\boldsymbol{p}_h. \tag{11}$$

The above relationship is used to estimate the stiffness of a human hand in certain postures in Section V.

IV. Numerical Analysis

This section presents numerical simulations of the asymmetric stiffness property of the upper limb shown in Fig. 3. Table I, II, III, and IV show the muscle properties and skeletal parameters used in the simulation. These parameters are basically determined with reference to [4].

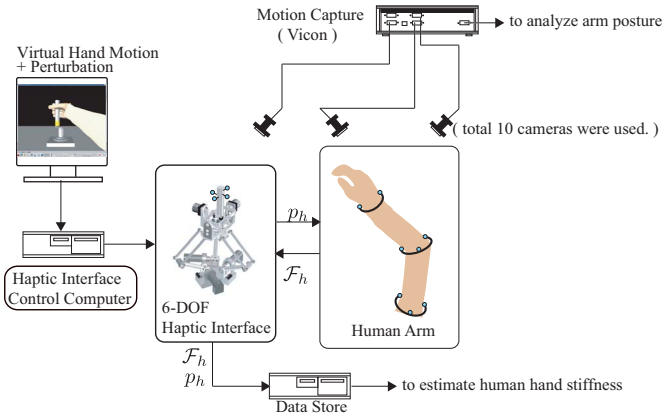

Fig. 6: Hand stiffness measurement system

Fig. 4 shows two simulation conditions. The left figure depicts the condition that the human intends to apply force onto $-x$ direction. The right figure depicts the condition that the human intends to apply force onto the opposite direction, namely $+x$ direction. This means that the human feels to push a stiff wall in a certain direction. The gray-colored region in the figure illustrates the virtual stiff wall. The thick blue and red arrows in the figure illustrate the direction of the force that human applied. In each condition, the perturbation is applied along arbitrary random directions as shown as the thinner black arrows.

Fig. 5 shows the simulated stiffness ellipses in the above two conditions. In the figure, left graph shows the case of the first condition and right graph shows the case of the second condition. The simulations were carried out with the asymmetric muscle model. As shown in the figure, the nonlinear stiffness properties are observed in different perturbation directions. Through these simulation results, two features are observed. Firstly, the size of the ellipse in the $+y$ area is larger than that in the other half area in the first condition, whereas the size of the ellipse in the $-y$ is larger than that in the other half area in the second condition. Secondly, due to the difference ratio of the muscle activation in the different conditions, the total size of the stiffness also varies in each condition. Note that the muscle activity level and the direction of the perturbation in muscle space are calculated based on the minimum norm solution in these simulations. The method to obtain the activity level and the direction of the perturbation in muscle space is still required to be considered in detail since the musculoskeltal system is redundant.

V. Stiffness Estimation Experiment

A. Experimental setup

To estimate the stiffness of the human hand, perturbation-excited-experiment was carried out. Three subjects (one male, two females) conducted in this experiment.

Fig. 6 shows the experimental setup for the estimation. A six DOF parallel robotic system as shown in Fig. 7 was used to apply the external displacement to the hand of the subject. The displacement and the reaction forces are

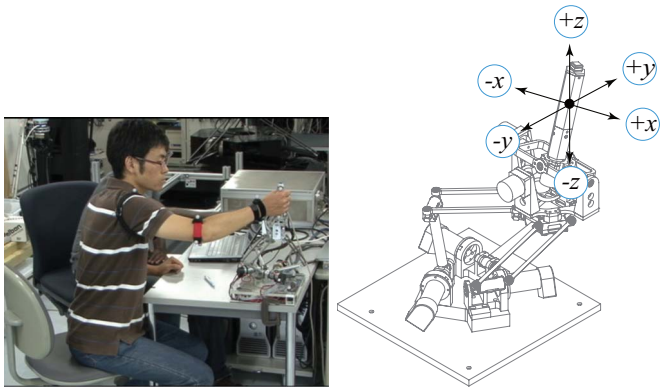

Fig. 7: Overview of the experimental setup

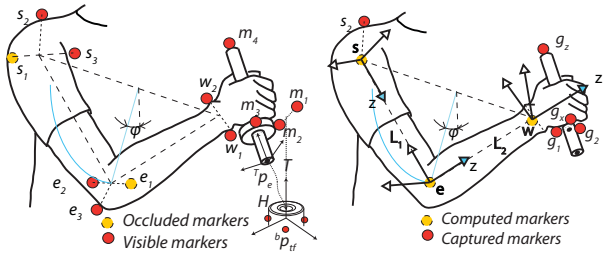

Fig. 8: Hand marker placement.

measured by encoders and a force/torque sensor attached on the robotic hand, respectively. The subject grasped the handle of the robotic system and maintained the posture during the experiment as shown in Fig. 7. In each trial, the subject intended to push the robotic handle to one direction. Fig. 11 shows the direction of force applied by the subject on xy plane (horizontal plane). By changing the applied force direction, the ratio of the muscle activation is varied. In the experiment, $10[mm]$ perturbation in $200[ms]$ period is randomly applied to six different directions ($\pm x$, $\pm y$, $\pm z$) as shown in Fig 7.

The posture of the human limb is observed by the motion capture system. Total 12 makers are attached on the limb of the subject. Fig. 8 shows the position of the attached markers. The position and orientation of each joint are calculated from the measured position of the markers.

B. Analysis of experimental result

Fig. 9 shows typical observed data from the estimation experiment. The top graph shows the external displacement along x axis. The bottom graph shows the external force displacement along x axis. In order to analyze the experimental results, first, one needs to comprehend causes of the reaction force against the perturbation. The reaction force is, in general, generated by voluntary and involuntary movements by a human. The voluntary movement is able to be produced after around $150[ms]$ by the high-level of central nervous system (CNS). The involuntary movement includes the intrinsic physical response and reflex phenomena. In the perturbation excitation onto the human hand, the stretch reflex is caused by a signal received the muscle spindle. When the spinal cord receives the stretch impulse,

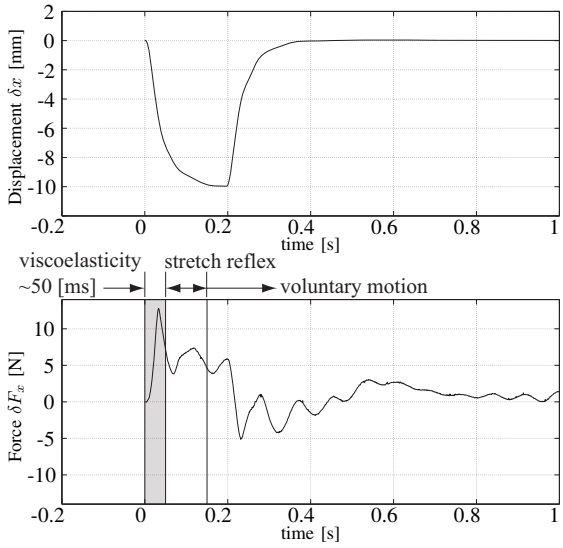

Fig. 9: Typical example of human hand displacement and reaction force

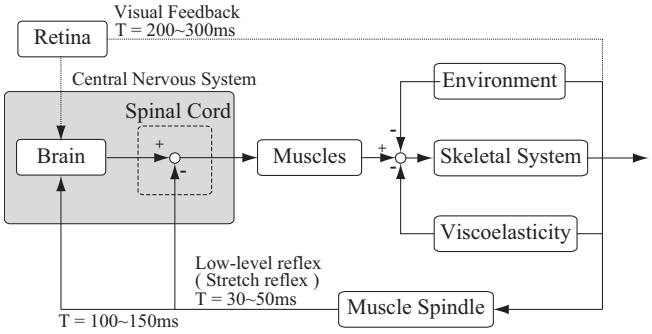

Fig. 10: Feedback loop of the nerve in motor system

a rapid muscle stretch sequence of events follows. However, the response of the stretch reflex generally delays about $30[ms]$ to $50[ms]$. Therefore, the reaction force observed within $50[ms]$ after the perturbation applied is pure physical intrinsic response of the hand. The observed data during this period are used to estimate the physical stiffness with the least square fitting method. Fig. 10 shows the feedback loop of the nerve in the motor system.

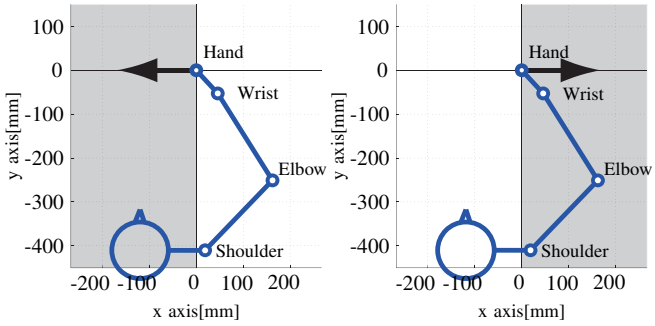

(a) Condition 1 (b) Condition 2

Fig. 11: Force direction applied by subject

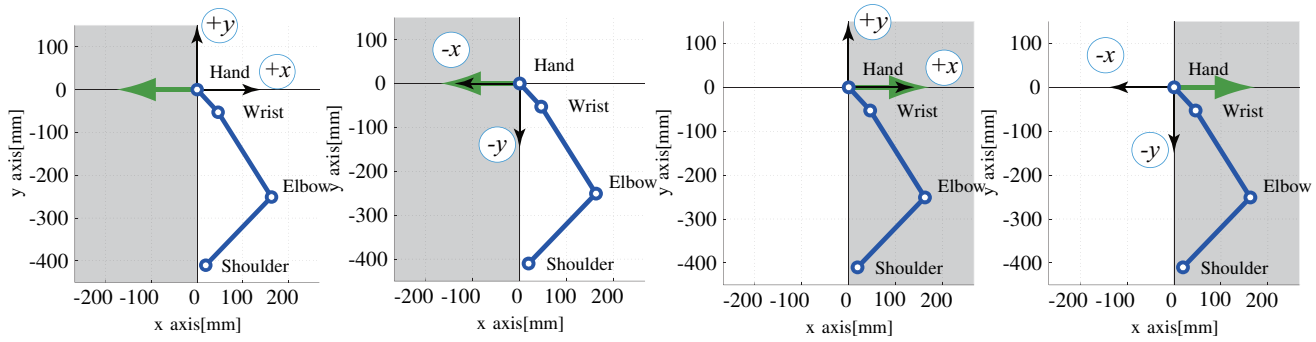

(a) Case 1 (b) Case 2 (c) Case 3 (d) Case 4

Fig. 12: Perturbation case with force applied by subject

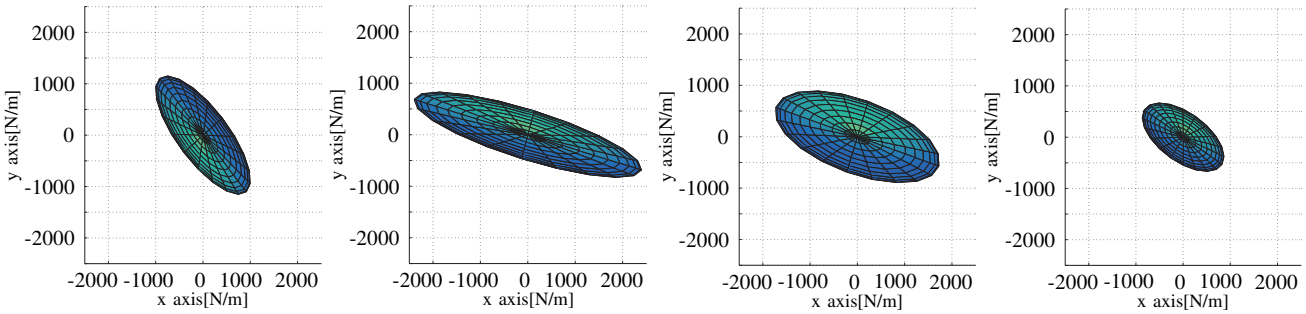

(a) xy plane (case 1) (b) xy plane (case 2) (a) xy plane (case 3) (b) xy plane (case 4)

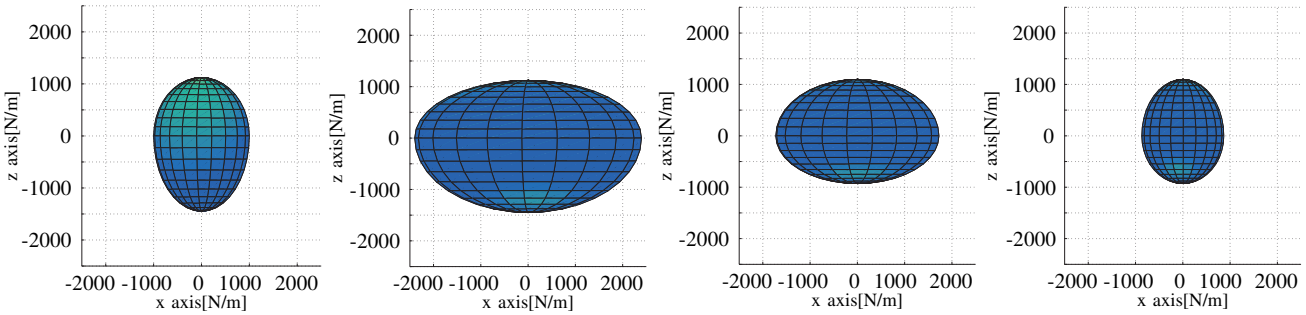

(c) xz plane (case 1) (d) xz plane (case 2) (c) xz plane (case 3) (d) xz plane (case 4)

Fig. 13: Stiffness ellipsoid in condition 1 (Subject 1)

Fig. 14: Stiffness ellipsoid in condition 2 (Subject 1)

C. Asymmetric stiffness ellipsoid

Figs. 13 and 14 show the estimated stiffness ellipsoids of one subject in one posture as shown in Fig. 11. Fig. 12 shows four cases of the perturbation directions with the force applied by the subject. The corresponding stiffness ellipsoids are shown in Figs. 13 and 14. Fig. 13 shows the case when the internal force is applied to $-x$ direction. Fig. 14 shows the case when the internal force is applied to $+x$ direction. The graphs (a) and (c) of each figure show the stiffness ellipsoids estimated from the data in the perturbations onto $+x$ and $+y$ directions. The graphs (b) and (d) show the stiffness ellipsoids estimated from the data in the perturbations onto $-x$ and $-y$ directions. The graph (a) and (b) are the results in xy plane, and the graph (c) and (d) are the results in xz plane, respectively. From the figures, it is observed that the estimated stiffness are different according to the perturbation direction. This results imply that the asymmetric stiffness characteristic exists in the muscle even in the same posture. In addition, the volume and orientation of the stiffness ellipsoids are different when the active internal force of the human arm is different. This results indicate that the human can change her/his hand

stiffness depending on the task as presented in the previous related researches [2], [3]. Additionally, it is shown that the strength of the muscles is different.

From the above analysis, new representation of the stiffness ellipsoid is presented in the following. Here, the stiffness is represented in four segmented quadrants on xy plane. In each quadrant on xy plane, stiffness is estimated by the measurement of the corresponding perturbation directions. Figs. 15, 16, and 17 show the asymmetric stiffness ellipsoids of each subject in two experimental conditions shown in Fig. 11. The results demonstrated that larger stiffness is observed on the direction where the agonist muscles are active than antagonist muscles. When the subject applied the force to $-x$ direction, the volume of the stiffness in the top half is larger than the bottom half region. On the other hand, the volume of the stiffness in the top half region is smaller than that in the bottom half region in the case when the subject applied the force to $+x$ direction. The above results imply that the stiffness of the muscle model is not symmetric. The proposed asymmetric stiffness model reproduces rather close stiffness characteristic of the human hand as the experimental results. Additionally, it seems that in the case when the force applied to $+x$ direction, the estimated stiffness ellipsoid is close to symmetric. However, it may occur because of the different strength of the flexor and extensor muscles.

Furthermore, along z axis, the magnitude of the stiffness is almost always larger in $-z$ direction than $+z$ direction. This effect is mainly obtained from the lower limb of the human limb. Therefore, further detail discussion is required by modeling the lower limb as well. Besides, the gravity force may influence the reaction force. It must be eliminated through dynamical analysis.

VI. Conclusions and Future Work

This paper presented the estimation of the stiffness characteristic of the human hand in a static posture. The experimental results implied that the stiffness property of the muscle model is not symmetric. This characteristic can not be explained only with the change of the muscle activity level in the conventional muscle model. This paper proposed an asymmetric stiffness model of the muscle model and compared the characteristic with the experimental results. The experimental results and the proposed asymmetric stiffness model provide close characteristic of the stiffness property of the human hand. The experimental results indicated that the human can optimally uses her/his muscles, not only depending on the task, but also the intensity of the task.

To comprehend more precise stiffness model, further experiment is required. As the future work, the electromyography (EMG) will be analyzed in detail during the experiment to find out precisely which muscles are active and how active they are. By combining the information with the forces observed on the hand and the electromyography, one will be able to identify more precise human muscle model. The muscle model is extended to a full three dimensional model and compare more accurately.

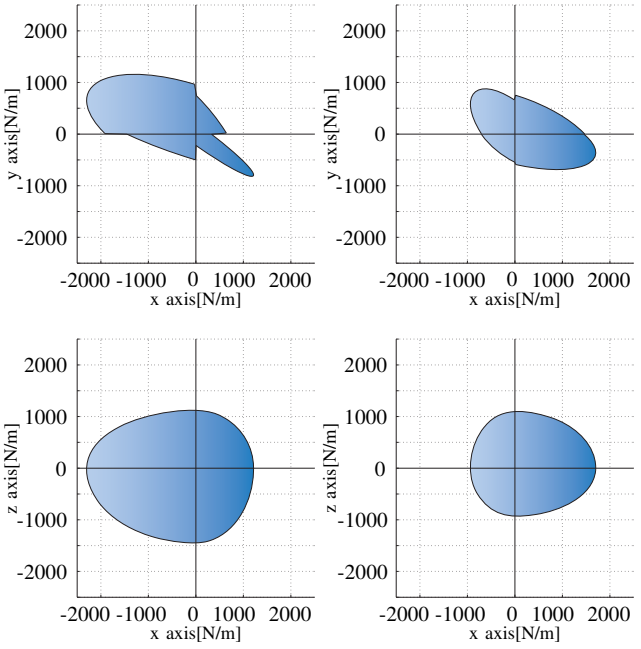

(a) Condition 1 (b) Condition 2

Fig. 15: Stiffness ellipsoid of subject 1

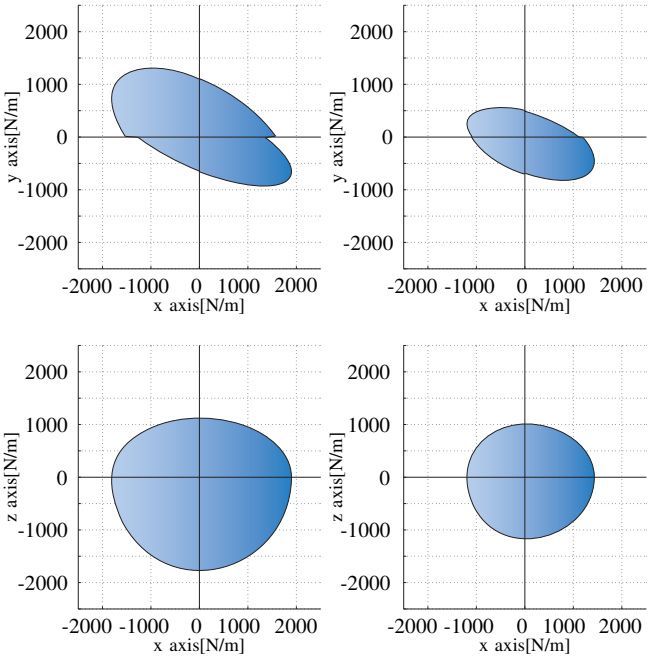

(a) Condition 1 (b) Condition 2

Fig. 16: Stiffness ellipsoid of subject 2

References

[1] N. Hogan, "The mechanics of multi-joint posture and movement control," *Biological Cybernetics*, vol. 52, pp. 315–331, 1985.

[2] T. Tsuji, P. G. Morasso, K. Goto, and K. Ito, "Human hand impedance characteristics during maintained posture," *Biological Cybernetics*, vol. 72, pp. 475 – 485, 1995.

[3] H. Gomi and R. Osu, "Task-dependent viscoelasticity of human mul-

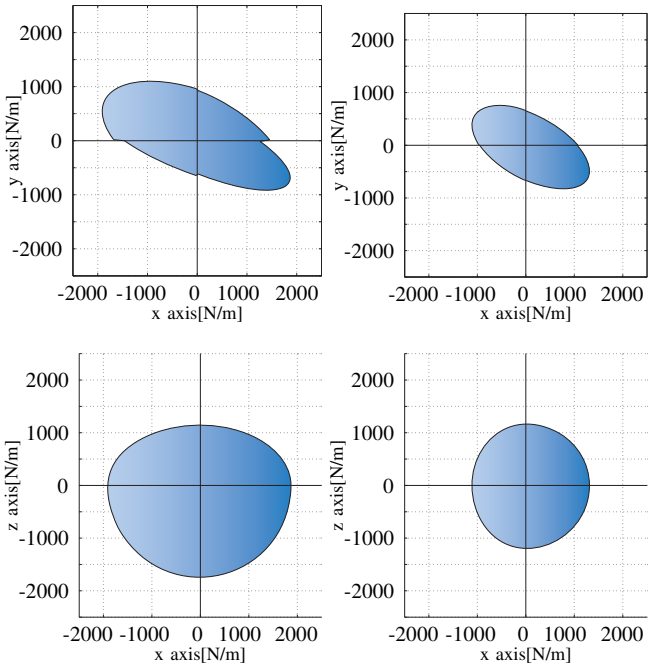

(a) Condition 1 (b) Condition 2

Fig. 17: Stiffness ellipsoid of subject 3

tijoint arm and its spatial characteristics for interaction with environments," *The Journal of Neuroscience*, vol. 18, no. 21, pp. 8965 – 8978, 1998.

[4] M. Katayama and M. Kawato, "Virtual trajectory and stiffness ellipse during multijoint arm movement predicted by neural inverse models," *Biological Cybernetics*, vol. 69, pp. 353 – 362, 1993.

[5] T. Flash and F. Mussa-Ivaldi, "Human arm stiff characteristics during the maintenance of posture," *Experimental Brain Research*, vol. 82, pp. 315 – 326, 1990.

[6] J. M. Dolan, M. B. Friedman, and M. L. Nagurka, "Dynamic and loaded impedance components in the maintenance of human arm posture," *IEEE Transactions on Systems, Man, and Cybernetics*, vol. 23, no. 3, pp. 698 – 709, 1993.

[7] K. Kosuge, Y. Fujisawa, and T. Fukuda, "Control of mechanical system with man-machine interaction," in *Proc. of the 1992 IEEE/RSJ International Conference on Intelligent Robots and Systems*, 1992, pp. 87 – 92.

[8] H. Asada and Y. Asari, "The direct teaching of tool manipulation skills via the impedance identification of human motions," in *Proc. of the 1998 IEEE International Conference on Robotics and Automation*.

[9] N. Hogan, "Adaptive control of mechanical impedance by coactivation of antagonist muscles," *IEEE Transactions on Automatic Control*, vol. AC-29, no. 8, pp. 681–690, 1984.